NASA Contractor Report 172307

STRESS INTENSITY FACTORS IN A REINFORCED THICK-WALLED CYLINDER

Renji Tang and F. Erdogan

LEHIGH UNIVERSITY
Bethlehem, Pennsylvania 18015

Grant NGR 39-007-011
February 1984

National Aeronautics and
Space Administration

Langley Research Center
Hampton, Virginia 23665

STRESS INTENSITY FACTORS IN A REINFORCED THICK-WALLED CYLINDER*

by

Renji Tang** and F. Erdogan

Lehigh University, Bethlehem, PA

Abstract

In this paper an elastic thick-walled cylinder containing a radial crack is considered. It is assumed that the cylinder is reinforced by an elastic membrane on its inner surface. The model is intended to simulate pressure vessels with cladding. The formulation of the problem is reduced to a singular integral equation. Various special cases including that of a crack terminating at the cylinder-reinforcement interface are investigated and numerical examples are given. Among the interesting results found one may mention the following: In the case of the crack touching the interface the crack surface displacement derivative is finite and consequently the stress state around the corresponding crack tip is bounded, and generally, for realistic values of the stiffness parameter, the effect of the reinforcement is not very significant.

1. Introduction

Because of its practical importance the problem of a thick-walled cylinder containing a radial crack has been studied rather extensively (see [1] for review and references). Considered as a plane problem the results obtained from such a study provide an upper bound for the stress intensity factors in pressure vessels, pipes, and disks containing an axial part-through crack. In all these previous studies it is assumed

(*) This work was supported by NSF under the Grant MEA-8209083 and by NASA-Langley under the Grant NGR 39-007-011.

(**) Visiting scholar. Permanent address: Associate Professor, Department of Mathematics and Mechanics, Lanzhou University, China.

that the cylinder is a homogeneous elastic solid. However, there is at least one group of technologically important problems in which the material may not be considered homogeneous. These are the problems which may generally be classified under "multi-layered" cylinders. Variety of reinforced disks and cylinders and pressure vessels with cladding may be cited as some examples. In this paper we are primarily interested in thick-walled cylinders with cladding containing a radial crack. This is a nonhomogeneous cylinder problem the distinguishing feature of which is that the thickness of the clad (that is, the inner cylinder) is very small compared to that of the main cylinder. The crack problem may be formulated and solved directly as a nonhomogeneous cylinder problem. However, there are at least two reasons for not following this procedure. First, the analysis of the nonhomogeneous problem is highly complicated and secondly if, as in the cladded pressure vessels, the thickness ratio of the two cylinders is very small, past experience indicate that there would be severe convergence problems in the related numerical calculations. In this paper the cladding will instead be approximated by a membrane and the problem will be treated as a reinforced thick-walled cylinder. A similar problem for a half plane and an infinite strip is considered in [2] and [3].

Introducing a dislocation into Mitchell's solution the problem is formulated in terms of a singular integral equation. The case of the crack terminating at the interface is separately studied and the stress intensity factors for various values of the stiffness constant characterizing the reinforcement are given.

2. The Basic Formulation

Except for the application of the boundary conditions, the formulation of the problem is quite similar to that given in [1]*. The stress state in the reinforced cylinder will again be expressed as the sum of two

(*) In this paper certain expressions have been simplified through further manipulations and by evaluating some of the series in closed form.

solutions containing the main features of the crack and the hollow cylinder, respectively. Omitting the details and referring to Figure 1 these two solutions may be written as follows (see [1] and [4]-[6]):

a. *The crack solution*

$$\sigma_{1rr}(r,\theta) = -\frac{2\mu}{\pi(\kappa+1)}\int_e^g [\frac{r\cos\theta-t-2t\sin^2\theta}{r^2+t^2-2rt\cos\theta} - \frac{2t^2\sin^2\theta(r\cos\theta-t)}{(r^2+t^2-2rt\cos\theta)^2}]f(t)dt, \tag{2.1}$$

$$\sigma_{1r\theta}(r,\theta) = \frac{2\mu}{\pi(\kappa+1)}\int_e^g [\frac{\sin\theta(2t\cos\theta-r)}{r^2+t^2-2rt\cos\theta} - \frac{2t\sin\theta(r\cos\theta-t)(r-t\cos\theta)}{(r^2+t^2-2rt\cos\theta)^2}]f(t)dt, \tag{2.2}$$

$$\sigma_{1\theta\theta}(r,) = -\frac{2\mu}{\pi(\kappa+1)}\int_e^g [\frac{2\cos\theta(r-t\cos\theta)+r\cos\theta-t}{r^2+t^2-2rt\cos\theta} - \frac{2(r\cos\theta-t)(r-t\cos\theta)^2}{(r^2+t^2-2rt\cos\theta)^2}]f(t)dt\ , \tag{2.3}$$

where μ is the shear modulus, $\kappa = 3-4\nu$ for plane strain, $\kappa = (3-\nu)/(1+\nu)$ for plane stress, ν the Poisson's ratio and the function f is defined by

$$f(r) = \frac{\partial}{\partial r}[u_\theta(r,+0) - u_\theta(r,-0)]\ ,\ (e<r<g)\ . \tag{2.4}$$

In order to facilitate the application of the boundary conditions, it is convenient to express the stress components on the boundary in terms of the following Fourier series:

$$\sigma_{1r\theta}(a,\theta) = \frac{\mu}{\pi(\kappa+1)}\int_e^g \sum_{n=1}^{\infty} A_n(t)\sin n\theta\ f(t)dt\ , \tag{2.5}$$

$$\sigma_{1rr}(a,\theta) = -\frac{\mu}{\pi(\kappa+1)}\int_e^g \sum_{n=0}^{\infty} B_n(t)\cos n\theta\ f(t)dt\ , \tag{2.6}$$

$$\sigma_{1\theta\theta}(a,\theta) = -\frac{\mu}{\pi(\kappa+1)}\int_e^g \sum_{n=0}^{\infty} C_n(t)\cos n\theta\, f(t)\, dt, \qquad (2.7)$$

$$\sigma_{1r\theta}(b,\theta) = \frac{\mu}{\pi(\kappa+1)}\int_e^g \sum_{n=1}^{\infty} D_n(t)\sin n\theta\, f(t)\, dt\ , \qquad (2.8)$$

$$\sigma_{1rr}(b,\theta) = -\frac{\mu}{\pi(\kappa+1)}\int_e^g \sum_{n=0}^{\infty} E_n(t)\cos n\theta\, f(t)\, dt\ . \qquad (2.9)$$

From (2.1)-(2.3) and (2.5)-(2.9) the Frouier coefficients may be obtained as follows:

$$B_0(t) = C_0(t) = -\frac{2}{t}\ ,\quad E_0(t) = -\frac{2}{b}\left(\frac{t}{b}\right)\ , \qquad (2.10)$$

$$A_1(t) = B_1(t) = \frac{1}{a}\left(\frac{a}{t}\right)^2,\ C_1(t) = -\frac{3}{a}\left(\frac{a}{t}\right)^2\ ,\ D_1(t) = -E_1(t) = \frac{1}{b}\left[3\left(\frac{t}{b}\right)^2 - 2\right], \qquad (2.11)$$

and

$$A_n(t) = \frac{1}{a}\left[n\left(\frac{a}{t}\right)^{n+1} - (n-2)\left(\frac{a}{t}\right)^{n-1}\right]\ ,\ B_n(t) = \frac{1}{a}\left[(n-2)\left(\frac{a}{t}\right)^{n+1} - (n-2)\left(\frac{a}{t}\right)^{n-1}\right)\ ,$$

$$C_n(t) = \frac{1}{a}\left[-(n+2)\left(\frac{a}{t}\right)^{n+1} + (n-2)\left(\frac{a}{t}\right)^{n-1}\right],\ D_n(t) = \frac{1}{b}\left[(n+2)\left(\frac{t}{b}\right)^{n+1} - n\left(\frac{t}{b}\right)^{n-1}\right],$$

$$E_n(t) = \frac{1}{b}\left[-(n+2)\left(\frac{t}{b}\right)^{n+1} + (n+2)\left(\frac{t}{b}\right)^{n-1}\right],\ (n = 2,3,\ldots)\ . \qquad (2.12)$$

b. *Michell's Solution*

If the loads satisfy the symmetry condition about the polar axis ox shown in Fig. 1, and the resultants of the tractions on the inner circular boundary r=a are zero, then the Michell's Solution for the hollow cylinder gives the following stress components [4], [1]

$$\sigma_{2rr}(r,\theta) = \int_e^g f(t)\{\frac{b_0}{r^2} + 2c_0 + (-\frac{2c_1}{r^3} + 2d_1 r)\cos\theta -$$

$$-\sum_{n=2}^{\infty}\left[a_n r^{n-2} + b_n(n-2)r^n + c_n r^{-n-2} + d_n(n+2)r^{-n}\right]\cos n\theta\}dt\ , \qquad (2.13)$$

$$\sigma_{2r\theta}(r,\theta) = \int_e^g f(t)\{(-\frac{2c_1}{r^3} + 2d_1 r)\sin\theta$$

$$+ \sum_{n=2}^{\infty} [a_n r^{n-2} + b_n n\, r^n - c_n r^{-n-2} - d_n n\, r^{-n}]\sin n\theta\}dt \ , \quad (2.14)$$

$$\sigma_{2\theta\theta}(r,\theta) = \int_e^g f(t)\{-\frac{b_0}{r^2} + 2c_0 + (\frac{2c_1}{r^3} + 6d_1 r)\cos\theta$$

$$+ \sum_{n=2}^{\infty} [a_n r^{n-2} + b_n(n+2)r^n + c_n r^{-n-2} + d_n(n-2)r^{-n}]\cos n\theta\}dt, \quad (2.15)$$

where a_n, b_n, c_n, and d_n $(n=0,1,\ldots)$ are functions of t and the constants

$$\int_e^g f(t)a_n(t)dt \ , \ \int_e^g f(t)b_n(t)dt \ , \ \ldots$$

replace the regular coefficients in the Mitchell's solution.

3. Boundary Conditions

Consider now a hollow elastic cylinder having radii a and b and containing a radial crack along $\theta = 0$, $e<r<g$ as shown in Figure 1. Assume that the inner boundary of the cylinder is reinforced by a thin membrane of thickness h and the self-equilibrating normal tractions on the crack surfaces are the only nonvanishing external loads.

Let the stress state in the cracked hollow cylinder be the sum of the two fundamental solutions given by (2.1)-(2.3) and (2.13)-(2.15), that is, let

$$\sigma_{ij}(r,\theta) = \sigma_{1ij}(r,\theta) + \sigma_{2ij}(r,\theta) \ , \ (i,j = r,\theta) \ . \quad (3.1)$$

Then the boundary conditions of the problem may be expressed as

$$\sigma_{1rr}(b,\theta) + \sigma_{2rr}(b,\theta) = 0, \ \ \sigma_{1r\theta}(b,\theta) + \sigma_{2r\theta}(b,\theta) = 0, \ (0\leq\theta<2\pi) \quad (3.2)$$

$$\sigma_{1rr}(a,\theta)+\sigma_{2rr}(a,\theta)=p_r(\theta)\ ,\quad \sigma_{1r\theta}(a,\theta)+\sigma_{2r\theta}(a,\theta)=p_\theta(\theta),\ (0\leq\theta<2\pi)$$

(3.3)

and

$$\sigma_{1\theta\theta}(r,\mp 0) + \sigma_{2\theta\theta}(r,\mp 0) = q(r)\ ,\ (e<r<g)\ , \tag{3.4}$$

where p_r and p_θ are the normal and shear tractions at the cylinder-reinforcement interface (Figure 1b). From the equilibrium of the membrane it may easily be shown that

$$p_r(\theta) = \sigma_{rr}(a,\theta) = \lambda\sigma_{\theta\theta}(a,\theta)\ ,\ (0\leq\theta<2\pi) \tag{3.5}$$

$$p_\theta(\theta) = \sigma_{r\theta}(a,\theta) = -\lambda\,\frac{\partial}{\partial\theta}\,\sigma_{\theta\theta}(a,\theta)\ ,\ (0\leq\theta<2\pi) \tag{3.6}$$

where

$$\lambda = \begin{cases} \dfrac{hE_m}{aE} & \text{for plane stress}\ , \\[2ex] \dfrac{E_m h(1-\nu^2)}{aE(1-\nu_m^2)+hE_m\nu(1+\nu)} & \text{for plane strain.} \end{cases} \tag{3.7}$$

In (3.7) E and ν are the elastic constants of the cylinder and E_m and ν_m of the reinforcing membrane.

By defining now

$$a_n = -\frac{\mu f(t)}{\pi(\kappa+1)}\,\alpha_n\ ,\ b_n = -\frac{\mu f(t)}{\pi(\kappa+1)}\,\beta_n\ ,$$

$$c_n = -\frac{\mu f(t)}{\pi(\kappa+1)}\,\gamma_n\ ,\ d_n = -\frac{\mu f(t)}{\pi(\kappa+1)}\,\delta_n,\ (n=0,1,\ldots) \tag{3.8}$$

and by substituting the stresses into the boundary conditions (3.2), (3.5) and (3.6) we obtain

$$\frac{\beta_0}{b^2} + 2\gamma_0 = E_0\ ,\ (1+\lambda)\,\frac{\beta_0}{a^2} + 2(1-\lambda)\gamma_0 = \lambda C_0 - B_0\ , \tag{3.9}$$

$$-\frac{2\gamma_1}{b^3}+2\delta_1 b=-E_1\ ,\quad 2(1+\lambda)\frac{\gamma_1}{a^3}+(6\lambda-2)\delta_1 a=B_1-\lambda C_1\ , \tag{3.10}$$

$$-\frac{2\gamma_1}{b^3}+2\delta_1 b=D_1\ ,\quad 2(1+\lambda)\frac{\gamma_1}{a^3}+(6\lambda-2)\delta_1 a=-A_1-\lambda C_1\ , \tag{3.11}$$

and

$$\alpha_n b^{n-2}+\beta_n(n-2)b^n+\gamma_n b^{-(n+2)}+\delta_n(n+2)b^{-n}=E_n \tag{3.12}$$

$$\alpha_n b^{n-2}+\beta_n\, n\, b^n-\gamma_n b^{-(n+2)}-\delta_n\, n\, b^{-n}=D_n \tag{3.13}$$

$$\alpha_n a^{n-2}(1+\lambda)+\beta_n a^n[(n-2)+\lambda(n+2)]+\gamma_n a^{-(n+2)}(1+\lambda)+\delta_n a^{-n}[(n+2)+\lambda(n-2)]$$

$$=B_n-\lambda C_n \tag{3.14}$$

$$\alpha_n a^{n-2}(1-n\lambda)+\beta_n a^n[n-\lambda n(n+2)]-\gamma_n a^{-(n+2)}(1+n\lambda)-\delta_n a^{-n}[n+\lambda n(n-2)]$$

$$=A_n+\lambda_n C_n \tag{3.15}$$

for $n=2,3,\ldots$. Note that A_i, B_i,... are known functions and are given by (2.10)-(2.12). Equations (3.10) and (3.11) imply that the constants A_1, B_1, D_1 and E_1 must satisfy

$$A_1+B_1=0\ ,\quad D_1+E_1=0\ . \tag{3.16}$$

It can be shown that equations (3.16) indeed follow from the fact that in the "crack solution" σ_{1ij} the self-equilibrating crack surface tractions are the only non-zero external loads and consequently the stress vector acting on $r=a$ has a zero resultant [1].

With (3.16), the solution of (3.9)-(3.11) is found to be

$$\beta_0=\frac{2(1-\lambda)a^2}{a^2(1-\lambda)-b^2(1+\lambda)}\left(t-\frac{b^2}{t}\right)\ , \tag{3.17}$$

$$\gamma_0=\frac{1}{a^2(1-\lambda)-b^2(1+\lambda)}\left[-(1+\lambda)t+\frac{a^2(1-\lambda)}{t}\right]\ , \tag{3.18}$$

$$\gamma_1 = \frac{a^4(1-3\lambda)}{a^4(1-3\lambda)-b^4(1+\lambda)}\left[-\frac{3t^2}{2} + b^2 + \frac{b^4}{2t^2}\right] , \tag{3.19}$$

$$\delta_1 = \frac{1}{a^4(1-3\lambda)-b^4(1+\lambda)}\left[-\frac{3(1+\lambda)t^2}{2} + b^2(1+\lambda) + \frac{a^4(1-3\lambda)}{2t^2}\right]. \tag{3.20}$$

Similarly, the solution of the infinite system (3.12)-(3.15) can be obtained as follows:

$$\alpha_n = b^{-2(n-1)}t^{n-1} - \beta_n(n-1)b^2 - \delta_n b^{-2(n-1)} , \tag{3.21}$$

$$\beta_n = \frac{\Delta_\beta}{\Delta_o} , \tag{3.22}$$

$$\gamma_n = \frac{1}{1+\lambda}\left[-a^{2(n+1)}t^{-(n+1)}(1-2n\lambda-\lambda)-\delta_n a^2(1+n-n\lambda-\lambda)+\beta_n a^{2(n+1)}(1-2n\lambda-\lambda)\right] , \tag{3.23}$$

$$\delta_n = \frac{\Delta_\delta}{\Delta_o} , \tag{3.24}$$

where the determinants Δ_o, Δ_β and Δ_δ are given by

$$\Delta_o = n^2(1+2\lambda+\lambda^2)a^{-2}b^2-2(n^2-1)(1-\lambda^2)-[1+2n\lambda+(2n-1)\lambda^2]a^{-2n}b^{2n}$$
$$- [1-2n\lambda-(2n+1)\lambda^2]a^{2n}b^{-2n} + n^2(1-2\lambda-3\lambda^2)a^2b^{-2} , \tag{3.25}$$

$$\Delta_\beta = \{(1-n^2)(1-\lambda^2)-[1-2n\lambda-(2n+1)\lambda^2]a^{2n}b^{-2n}+n^2(1-2\lambda-3\lambda^2)a^2b^{-2}\}t^{-(n+1)}$$
$$+ \{(2+n-n^2)(1-\lambda^2)b^{-2}-(2+n-n^2)(1+2\lambda+\lambda^2)a^{-2}\}t^{-(n-1)}+\{(1+n)[1+2n\lambda-(1-2n)\lambda^2]a^{-2n}$$
$$-(1+n)(1-\lambda^2)b^{-2n}\}t^{n-1}+\{(2+n)(1+2\lambda+\lambda^2)a^{-2}b^{-2n}$$
$$-(2+n)[1+2n\lambda-(1-2n)\lambda^2]a^{-2n}b^{-2}\}t^{n+1} , \tag{3.26}$$

$$\Delta_\delta = \{-(1-n)[1-2n\lambda-(1+2n)\lambda^2]a^{2n}+(1-n)(1-\lambda^2)b^{2n}\}t^{-(n+1)}-\{(2-n)(1+2\lambda+\lambda^2)a^{-2}b^{2n}$$

$$-(2-n)[1-2n\lambda-(1+2n)\lambda^2]a^{2n}b^{-2}\}t^{-(n-1)}+\{n^2(1+2\lambda+\lambda^2)a^{-2}b^2+(1-n^2)(1-\lambda^2)$$

$$-[1-2n\lambda-(1+2n)\lambda^2]a^{2n}b^{-2n}\}t^{n-1}+\{(2-n-n^2)(1+2\lambda+\lambda^2)a^{-2}-(2-n-n^2)(1-\lambda^2)b^{-2}\}t^{n+1}. \tag{3.27}$$

4. The Integral Equation

Having determined α_n, β_n, γ_n, and δ_n, from (3.8) and from the expressions for stresses it is seen that the solution of the cracked cylinder problem is completely known in terms of the crack surface displacement derivative $f(r)$. This function is as yet unknown and may be determined by using the remaining boundary condition (3.4). Thus, by substituting the stresses $\sigma_{1\theta\theta}$ and $\sigma_{2\theta\theta}$ as expressed in terms of $f(r)$ into (3.4), after some manipulations and separating the singular part of the kernel we obtain the following integral equation:

$$\int_e^g \frac{f(t)}{t-r}\,dt + \int_e^g k(r,t)f(t)dt = -\frac{\pi(1+\kappa)}{2\mu}\,q(r), \quad e<r<g\ , \tag{4.1}$$

where the bounded kernel $k(r,t)$ is given by

$$k(r,t) = -\frac{1}{2}\{-\frac{\beta_0}{r^2} + 2\gamma_0 + \frac{2\gamma_1}{r^3} + 6\delta_1 r$$

$$+ \sum_{n=2}^{\infty}[\alpha_n r^{n-2} + \beta_n(n+2)r^n + \gamma_n r^{-(n+2)} + \delta_n(n-2)r^{-n}]\} \tag{4.2}$$

From the definition of $f(r)$ as given by (2.4) it is seen that the following singlevaluedness condition must be satisfied

$$\int_e^g f(r)dr = 0\ . \tag{4.3}$$

The singular integral equation (4.1) may easily be solved numerically by using the procedure outlined, for example, in [7]. Noting that the solution of (4.1) is of the form [8]

$$f(r) = F(r)/\sqrt{(r-e)(g-r)} \quad , \tag{4.4}$$

where $F(r)$ is a bounded function, after determining $f(r)$ the stress intensity factors at the crack tips may be defined and evaluated as follows:

$$k(e) = \lim_{r\to e} \sqrt{2(e-r)}\ \sigma_{\theta\theta}(r,0) = \lim_{r\to e} \frac{2\mu}{1+\kappa} \sqrt{2(r-e)}\ f(r) \quad , \tag{4.5}$$

$$k(g) = \lim_{r\to g} \sqrt{2(r-g)}\ \sigma_{\theta\theta}(r,0) = -\lim_{r\to g} \frac{2\mu}{1+\kappa} \sqrt{2(g-r)}\ f(r) \quad . \tag{4.6}$$

5. Special Cases

The first special case to be considered is an infinite plane which contains a reinforced circular hole and a finite radial crack. In this case by letting $b\to\infty$ the Fredholm kernel $k(r,t)$ in (4.1) may be simplified as

$$\lim_{b\to\infty} k(r,t) = k_1(r,t) = -\frac{1}{2}\left\{-\frac{\beta_0}{r^2} + \frac{2\gamma_1}{r^3} + \sum_{n=2}^{\infty} [\gamma_n r^{-(n+2)} + \delta_n (n-2) r^{-n}]\right\} \quad , \tag{5.1}$$

$$\beta_0 = \frac{2a^2}{t} \quad , \quad \gamma_1 = -\frac{a^4(1-3\lambda)}{2(1+\lambda)} \frac{1}{t^2} \quad , \tag{5.2}$$

$$\gamma_n = -\frac{a^{2(n+1)}(n^2-3\lambda n^2)}{2\lambda n + 1 - \lambda} \cdot \frac{1}{t^{n+1}} + \frac{a^{2n}(n^2-n-2-\lambda n^2+\lambda n+2\lambda)}{2\lambda n+1-\lambda} \cdot \frac{1}{t^{n-1}} \quad , \tag{5.3}$$

$$\delta_n = \frac{a^{2n}(n-\lambda n-1+\lambda)}{2\lambda n+1-\lambda} \cdot \frac{1}{t^{n+1}} - \frac{a^{2(n-1)}(n-2+\lambda n-2\lambda)}{2\lambda n+1-\lambda} \cdot \frac{1}{t^{n-1}} \quad . \tag{5.4}$$

Note that the new kernel given by (5.1) can be evaluated partly in closed form by using the following infinite series:

$$Ax + (A+B)x^2 + (A+2B)x^3 + \ldots = \frac{Ax + (B-A)x^2}{(1-x)^2} \tag{5.5}$$

where A and B are arbitrary constants.

After some obvious transformations it can be shown that

$$\begin{aligned} k_1(r,t) = -\frac{1}{2}\{ & -\frac{\beta_0}{r^2} + \frac{2\gamma_1}{r^3} + \frac{1}{4}\left(\frac{15a^6}{r^3t^2} - \frac{3a^4}{r^3} + \frac{a^4}{rt^2} + \frac{3a^2}{r}\right)\frac{1}{rt-a^2} \\ & + \frac{1}{2}\left(\frac{3a^6}{r^3t^2} - \frac{a^4}{r^3} - \frac{a^4}{rt^2} - \frac{a^2}{r}\right)\frac{a^2}{(rt-a^2)^2} - \frac{1}{4}\left(\frac{3a^4}{r^3t^2} + \frac{9a^2}{r^3} - \frac{3a^2}{rt^2}\right. \\ & \left. + \frac{23}{r}\right)\sum_{n=2}^{\infty}\frac{1}{2\lambda n+1-\lambda}\left(\frac{a^2}{rt}\right)^{n-1} - \left(\frac{a^4}{r^3t^2} - \frac{a^2}{r^3} - \frac{a^2}{r^2t} + \frac{1}{r}\right)\cdot\sum_{n=2}^{\infty}\frac{n^2}{2\lambda n+1-\lambda} \\ & \cdot\left(\frac{a^2}{rt}\right)^{n-1} - \frac{1}{2}\left(\frac{3a^4}{r^3t^2} + \frac{a^2}{r^3} + \frac{5a^2}{rt^2} - \frac{9}{r}\right)\sum_{n=2}^{\infty}\frac{n}{2\lambda n+1-\lambda}\left(\frac{a^2}{rt}\right)^{n-1} + \frac{1}{4}\left(\frac{3a^4}{r^3t^2}\right. \\ & \left. + \frac{9a^2}{r^3} - \frac{3a^2}{rt^2} - \frac{9}{r}\right)\sum_{n=2}^{\infty}\frac{\lambda}{2\lambda n+1-\lambda}\left(\frac{a^2}{rt}\right)^{n-1} . \end{aligned} \tag{5.6}$$

Now observing that

$$\sum_{n=2}^{\infty}\frac{1}{2\lambda n+1-\lambda}\left(\frac{a^2}{rt}\right)^{n-1} = \frac{rt}{2\lambda a^2}\sum_{n=2}^{\infty}\frac{1}{n}\left(\frac{a^2}{rt}\right)^{n} - \frac{(1-\lambda)}{2\lambda}\sum_{n=2}^{\infty}\frac{1}{n(2n\lambda+1-\lambda)}\left(\frac{a^2}{rt}\right)^{n-1} , \tag{5.7}$$

and

$$\log\left(\frac{1}{1-x}\right) = \sum_{1}^{\infty}\frac{x^n}{n} \quad , \quad -1\leq x<1 , \tag{5.8}$$

the kernel $k_1(r,t)$ may be decomposed as follows:

$$k_1(r,t) = k_{1s}(r,t) + k_{1ws}(r,t) + k_{1b}(r,t) \tag{5.9}$$

where

where

$$k_{1s}(r,t) = -\frac{1}{8}\left(\frac{15a^6}{r^3t^2} - \frac{3a^4}{r^3} + \frac{a^4}{rt^2} + \frac{3a^2}{r}\right)\frac{1}{rt-a^2}$$

$$-\frac{1}{4}\left(\frac{3a^6}{r^3t^2} - \frac{a^4}{r^3} - \frac{a^4}{rt^2} - \frac{a^2}{r}\right)\frac{a^2}{(rt-a^2)^2}\,, \qquad (5.10)$$

$$k_{1ws}(r,t) = -\frac{rt}{16a^2\lambda}\left(\frac{3a^4}{r^3t^2} + \frac{9a^2}{r^3} - \frac{3a^2}{rt^2} + \frac{23}{r}\right)\log(rt-a^2) \qquad (5.11)$$

$$k_{1b}(r,t) = \frac{1}{8}\left(\frac{3a^4}{r^3t^2} + \frac{9a^2}{r^3} - \frac{3a^2}{rt^2} + \frac{23}{r}\right)\left[\frac{rt}{2a^2\lambda}\log rt\right.$$

$$-\frac{1}{2\lambda} - \sum_{n=2}^{\infty}\frac{(1-\lambda)\left(\frac{a^2}{rt}\right)^{n-1}}{2\lambda n(2\lambda n+1-\lambda)}$$

$$-\frac{1}{2}\left\{-\frac{\beta_0}{r^2} + \frac{2\gamma_1}{r^3} - \left(\frac{a^4}{r^3t^2} - \frac{a^2}{r^3} - \frac{a^2}{rt^2} + \frac{1}{r}\right)\sum_{n=2}^{\infty}\frac{n^2\left(\frac{a^2}{rt}\right)^{n-1}}{2\lambda n+1-\lambda}\right.$$

$$-\frac{1}{2}\left(\frac{3a^4}{r^3t^2} + \frac{a^2}{r^3} + \frac{5a^2}{rt^2} - \frac{9}{r}\right)\sum_{n=2}^{\infty}\frac{n\left(\frac{a^2}{rt}\right)^{n-1}}{2\lambda n+1-\lambda}$$

$$+\frac{1}{4}\left(\frac{3a^4}{r^3t^2} + \frac{9a^2}{r^3} - \frac{3a^2}{rt^2} - \frac{9}{r}\right)\sum_{n=2}^{\infty}\frac{\lambda\left(\frac{a^2}{rt}\right)^{n-1}}{2\lambda n+1-\lambda} \qquad (5.12)$$

The subscripts in k_{1s}, k_{1ws} and k_{1b} refer to the fact that as r and t both approach e = a (in the case of the crack touching the interface), these kernels become "singular", "weakly singular" and "bounded", respectively.

The second special case is that of an infinite plane containing a radial crack and a circular hole without reinforcement. In this case by letting $\lambda = 0$ (see (3.7)) it can be shown that the kernel k(r,t) in (4.1) may be evaluated in closed form as follows:

$$\lim_{\substack{b\to\infty\\ \lambda\to 0}} k(r,t) = k_2(r,t) = -\frac{(t^2-a^2)^2a^2}{t(rt-a^2)^3} + \frac{t(t^2-a^2)}{(rt-a^2)^2} + \frac{t}{rt-a^2} + \frac{a^2-t^2}{r^2t} - \frac{a^2}{r^3} - \frac{1}{r}\,. \qquad (5.13)$$

The third special case refers to the infinite plane with a reinforced circular hole and a radial crack in which the radius a is infinitely large. This is the problem of a cracked half plane reinforced by a membrane along its boundary (Figure 2). In this case if we define

$$r = a + y,\ t = a + \zeta\ ,\ e = a + e_o,\ g = a + g_o\ , \tag{5.14}$$

and assume that y and ζ remains finite as a tends to infinity, the kernel $k(r,t)$ in (4.1) becomes

$$k(r,t)\Big|_{\substack{b\to\infty\\ a\to\infty}} = \lim_{a\to\infty} k_1(a+y,a+\zeta) = k_3(y,\zeta),\ (e_o<(y,\zeta)<g_o)\ . \tag{5.15}$$

Again, by evaluating the asymptotically dominant terms in the infinite series in closed form, after somewhat lengthy manipulations we obtain

$$k_3(y,\zeta) = -\frac{1}{\zeta+y} - \frac{2\zeta+y}{\phi h(\zeta+y)} - \frac{\zeta y}{2\phi^2h^2(\zeta+y)} + \frac{\zeta y}{\phi h(\zeta+y)^2}$$
$$+ \left(4 + \frac{\zeta y}{2\phi^2h^2} + \frac{2\zeta+y}{\phi h}\right)\cdot \lim_{a\to\infty} \sum_{n=2}^{\infty} \frac{\left(1 - \frac{\zeta+y}{a}\right)^{n-1}}{2\phi hn + a} \tag{5.16}$$

where

$$\phi = \begin{cases} E_m/E \quad \text{for plane stress,} \\ E_m(1-\nu^2)/E(1-\nu_m^2) \quad \text{for plane strain .} \end{cases} \tag{5.17}$$

Of course, the integral equation for the half plane problem may also be derived directly by using the method of Fourier transforms. By following this technique and by omitting the details, after evaluating the asymptotically dominant infinite integrals, the kernel $k_3(y,\zeta)$ may be obtained as follows:

$$k_3(y,\zeta) = -\frac{1}{\zeta+y} - \frac{2\zeta+y}{\phi h(\zeta+y)} - \frac{\zeta y}{2\phi^2h^2(\zeta+y)} + \frac{\zeta y}{\phi h(\zeta+y)^2}$$
$$+ \left(4 + \frac{\zeta y}{2\phi^2h^2} + \frac{2\zeta+y}{\phi h}\right)\cdot \int_0^{\infty} \frac{e^{-(\zeta+y)\alpha}}{2\phi h\alpha + 1}\, d\alpha\ . \tag{5.18}$$

Finally, for the half plane without reinforcement it can be shown that for $a\to\infty$ (5.13) would reduce to the following known kernel [7]

$$k_4(y,\zeta) = -\frac{1}{\zeta+y} + \frac{6y}{(\zeta+y)^2} - \frac{4y^2}{(\zeta+y)^3} \quad . \tag{5.19}$$

6. The Case of the Crack Touching The Interface (e=a)

In the infinite plane containing a reinforced circular hole considered in the previous section, let us assume that the inner crack tip touches the interface, (i.e., e=a). In this case, from (5.9)-(5.12) the kernel $k(r,t)$ of the integral equation (4.1) may be shown to reduce to

$$\lim_{\substack{b\to\infty \\ e\to a}} k(r,t) = \tilde{k}_1(r,t) = \tilde{k}_{1s}(r,t) + \tilde{k}_{1ws}(r,t) + \tilde{k}_{1b}(r,t) \tag{6.1}$$

$$\tilde{k}_{1s}(r,t) = \frac{1}{8}\left(\frac{3a^4}{r^4} - \frac{6a^2}{r^2} - 5\right)\frac{1}{t-\frac{a^2}{r}} + \frac{a^2(r+a)^2(r-a)^2}{4r^5}\cdot\frac{1}{(t-\frac{a^2}{r})^2} \tag{6.2}$$

$$\tilde{k}_{1ws}(r,t) = -\frac{rt}{16a^2\lambda}\left(\frac{3a^4}{r^3t^2} + \frac{9a^2}{r^3} - \frac{3a^2}{rt^2} + \frac{23}{r}\right)\log(rt-a^2) \tag{6.3}$$

$$\tilde{k}_{1b}(r,t) = k_{1b}(r,t) + \frac{1}{8t}\left(\frac{3a^2}{r^2} + 5\right) + \frac{1}{8t^2}\left(\frac{9a^4}{r^3} + \frac{3a^2}{r}\right). \tag{6.4}$$

Note that as both r and t approach the interface r = a, the kernel $\tilde{k}_{1s}$ become unbounded and hence influence the singular behavior of the solution f(t). This behavior may be investigated by letting

$$f(t) = (g-t)^{-\alpha}(t-a)^{-\beta} \ , \ (0<\mathrm{Re}(\alpha,\beta)<1) \tag{6.5}$$

and by using the function theoretic method described in [7]. Omitting the details, the characteristic equations giving α and β may thus be obtained as

$$\cos\pi\alpha = 0 \quad , \quad \cot\pi\beta - \frac{1}{\sin\pi\beta} = 0 \ , \tag{6.6}$$

giving $\alpha = 1/2$ and $\beta = 0$ as the acceptable roots. The root $\beta = 0$ indicate that at the crack tip $r = a$ the crack surface derivative is finite. Since the bending stiffness of the reinforcement is zero, this is the physically expected result.

In the limiting case of $a \to \infty$ (Figure 2), the kernel given by (5.18) which is obtained from the method of Frouier transforms is still valid. In this case the integral in (5.18) may be evaluated as

$$\int_0^\infty \frac{e^{-(\zeta+y)\alpha}}{2\phi h\alpha+1}\, d\alpha = -\frac{e^{-\theta}}{2\phi h}\left[E_o+\log\left(\frac{\zeta+y}{2\phi h}\right) + \sum_1^\infty \frac{\theta^n}{n\cdot n!}\right], \tag{6.7}$$

where $\theta = -(\zeta+y)/2\phi h$ and $E_o = 0.5772157$ is the Euler's constant. Hence the infinite integral in (5.18) has the following order:

$$\int_0^\infty \frac{e^{-\alpha(\zeta+y)}}{2\phi h\alpha+1}\, d\alpha \sim O[\log(\zeta+y)] \tag{6.8}$$

and the kernel of the integral equation (4.1) may be arranged as follows:

$$k(r,t) = \tilde{k}_3(y,\zeta) = \tilde{k}_{3s}(y,\zeta) + \tilde{k}_{3ws}(y,\zeta) + \tilde{k}_{3b}(y,\zeta)\ , \tag{6.9}$$

$$\tilde{k}_{3s}(y,\zeta) = -\frac{1}{\zeta+y}\ , \tag{6.10}$$

$$k_{3ws}(y,\zeta) = 4\int_0^\infty \frac{e^{-\alpha(\zeta+y)}}{2\phi h\alpha+1}\, d\alpha\ , \tag{6.11}$$

$$\tilde{k}_{3b}(y,\zeta) = -\frac{2\zeta+y}{\phi h(\zeta+y)} - \frac{\zeta y}{2\phi^2h^2(\zeta+y)} + \frac{\zeta y}{\phi h(\zeta+y)^2} + \left(\frac{\zeta y}{2\phi^2h^2} + \frac{2\zeta+y}{\phi h}\right)\int_0^\infty \frac{e^{-\alpha(\zeta+y)}}{2\phi h\alpha+1}\, d\alpha\ . \tag{6.12}$$

It is seen that as ζ and y both approach zero $\tilde{k}_{3s}$ becomes unbounded, $\tilde{k}_{3ws}$ exhibits only a weak singularity and $\tilde{k}_{3b}$ remains unbounded.

Thus, if we express f(t) again as in (6.5), the function theoretic method gives the characteristic equations for α and β as

$$\cos \pi\alpha = 0 \ , \ (\cos\pi\beta-1)/\sin\pi\beta = 0 \tag{6.13}$$

which are the same as (6.6) and give $\alpha = 1/2$ and $\beta = 0$. This result could also be obtained from the circular hole problem by substituting $r = a+y$, $t = a+\zeta$, and by letting $a\to\infty$ in (6.2). After some simple algebra one may then observe that the principal part of the kernel $\tilde{k}_{1s}$ is $-1/(\zeta+y)$ which is identical to (6.10).

7. Solution and Results

Excepting the problem of unreinforced edge crack, in all cases considered the displacement u_θ at the crack tips is zero and consequently the integral equation (4.1) and all its special cases must be solved under the single-valuedness condition (4.3). For the numerical solution following normalized quantities are introduced:

$$t = \frac{g-e}{2}\tau + \frac{g+e}{2} \ , \ r = \frac{g-e}{2}\rho + \frac{g+e}{2} \ , \tag{7.1}$$

$$\tilde{k}(\rho,\tau) = \frac{g-e}{2} k(r,t) \ , \ \tilde{q}(\rho) = q(r) \ , \tag{7.2}$$

$$\tilde{f}(\tau) = \frac{2\mu}{\kappa+1} f(t) = \tilde{F}(\tau)w(\tau) \ , \ (-1<\tau<1) \ . \tag{7.3}$$

In the embedded crack problem (i.e., for e>a) $w(\tau) = (1-\tau^2)^{-1/2}$ and a Gauss-Chebyshev integration technique is used to determine $\tilde{F}(\tau)$ [7]. The stress intensity factors are then evaluated from (see (4.5) and (4.6))

$$k(e) = \sqrt{(g-e)/2}\ \tilde{F}(-1) \ , \ k(g) = -\sqrt{(g-e)/2}\ \tilde{F}(1). \tag{7.4}$$

For e=a the function f(r) is bounded at r=a, (i.e. in (6.5) β=0) and the stress intensity factor at r=g is obtained from

$$k(g) = -\sqrt{g-a}\ \tilde{F}(1) \ . \qquad (7.5)$$

The calculated stress intensity factors are given in Tables 1-6. In the case of an embedded crack (i.e., for e>a or e_o>0) the stress intensity factors are normalized as follows:

$$\frac{k(e)}{q_o\sqrt{(g-e)/2}} = k_n(e) \ , \ \frac{k(g)}{q_o\sqrt{(g-a)/2}} = k_n(g) \ . \qquad (7.6)$$

Table 1 gives an example showing the effect of the stiffness parameter λ defined by (3.7) on the stress intensity factors. Similar results for a reinforced half plane are shown in Table 2. The stiffness constant ϕ shown in Table 2 is defined by (5.17).

The results for somewhat more realistic values of the stiffness parameter λ and the radius ratio a/b which may simulate a pressure vessel with internal cladding are shown in Table 3-6. The normalized stress intensity factors are calculated for two types of external loads. In the first it is assumed that a uniform crack surface pressure $\sigma_{\theta\theta}(r,0) = q(r) = -q_o$ is the only nonzero applied load. In the second the cylinder is assumed to be under internal pressure $\sigma_{rr}(a-h,\theta) = -p_o$.

Generally, for the embedded crack the influence of the membrane reinforcement or the cladding on the stress intensity factors does not seem to be very significant. Since the properties of the clad material cannot be very different than that of the cylinder, this result is not surprising. However, in the case of the crack terminating at the interface (i.e., for e=a, Figure 1) the stress intensity factors k(g) calculated for $\lambda \neq 0$ and $\lambda = 0$ are very different. For $\lambda = 0$ there is no reinforcement and the crack is an edge crack with a non-zero opening at r=a (i.e., $u_\theta(a,+0)-u_\theta(a,-0)>0$). On the other hand, for $\lambda \neq 0$ since $u_\theta(a,0)=0$ there is a great deal of constraint tending to reduce the stress intensity factor. One may note that because of the membrane assumption made for the reinforcement at r=a the derivative of the crack surface displacement is finite giving a finite angle between the upper and lower crack surfaces.

Table 1. Stress intensity factors in a reinforced hollow circular cylinder containing a radial crack (Figure 1). External load: uniform crack surface pressure $q(r) = -q_0$, $a = 0.5b$, $g-e = 0.5(b-a)$, $k_n(e) = k(e)/q_0\sqrt{(g-e)/2}$, $k_n(g) = k(g)/q_0\sqrt{(g-e)/2}$.

$\frac{e-a}{b-a}$	$\lambda = 0$		$\lambda = 0.2$		$\lambda = 0.5$	
	$k_n(e)$	$k_n(g)$	$k_n(e)$	$k_n(g)$	$k_n(e)$	$k_n(g)$
0.15	1.1968	1.1754	1.1085	1.1255	1.0549	1.0988
0.20	1.1517	1.1769	1.1123	1.1436	1.0740	1.1223
0.25	1.1331	1.1951	1.1215	1.1706	1.0926	1.1523
0.30	1.1727	1.2303	1.1379	1.2100	1.1148	1.1930
0.35	1.1893	1.2912	1.1637	1.2702	1.1439	1.2526
0.40	1.2263	1.4033	1.2042	1.3764	1.1854	1.3559

Table 2. Stress intensity factors in a reinforced half plane containing a crack perpendicular to the boundary (Figure 2). External load: uniform crack surface pressure $q(y) = -q_o$, $\lambda_o = h\phi/g$, $k_n(g_o) = k(g_o)/q_o\sqrt{(g_o-e_o)/2}$, $k_n(e_o) = k(e_o)/q_o\sqrt{(g_o-e_o)/2}$.

e_o/g_o	$\lambda_o = 0$		$\lambda_o = 0.0375$		$\lambda_o = 0.075$		$\lambda_o = 0.15$		$\lambda_o = 0.3$	
	$k_n(e_o)$	$k_n(g_o)$	$k_n(e_o)$	$k_n(g_o)$	$k_n(e_o)$	$k_n(g_o)$	$k_n(e_o)$	$k_n(g_o)$	$k_n(e_o)$	$k_n(g_o)$
0.1	1.42667	1.15500	1.41438	1.15234	1.40300	1.14983	1.38222	1.14510	1.34633	1.13661
0.2	1.20354	1.09670	1.19970	1.09543	1.19604	1.09422	1.18921	1.09190	1.17698	1.08765
0.3	1.11075	1.06242	1.10909	1.06171	1.10750	1.06103	1.10449	1.05972	1.09902	1.05730
0.4	1.06224	1.03990	1.06145	1.03949	1.06068	1.03909	1.05923	1.03833	1.05655	1.03691

Table 3. Stress intensity factors in a reinforced hollow circular cylinder containing a radial crack (Figure 1). External load: uniform crack surface pressure $q(r) = -q_o$, $a/b = 0.8$, $e/a = 1.05$, $k_n(g) = k(g)/q_o\sqrt{(g-e)/2}$, $k_n(e) = k(e)/q_o\sqrt{(g-e)/2}$.

$\frac{g-e}{b-a}$	$\lambda = 0$		$\lambda = 0.001$		$\lambda = 0.002$		$\lambda = 0.004$	
	$k_n(e)$	$k_n(g)$	$k_n(e)$	$k_n(g)$	$k_n(e)$	$k_n(g)$	$k_n(e)$	$k_n(g)$
0.05	1.0044	1.0041	1.0043	1.0039	1.0042	1.0038	1.0039	1.0036
0.10	1.0157	1.0133	1.0153	1.0129	1.0148	1.0126	1.0140	1.0119
0.20	1.0511	1.0382	1.0497	1.0373	1.0484	1.0364	1.0459	1.0349
0.30	1.0962	1.0668	1.0938	1.0656	1.0915	1.0644	1.0871	1.0621
0.40	1.1466	1.1023	1.1432	1.1011	1.1400	1.0998	1.1339	1.0974
0.50	1.2021	1.1596	1.1979	1.1584	1.1940	1.1573	1.1866	1.1552

Table 4. Stress intensity factors in a reinforced pressurized cylinder containing a radial crack. External load: internal pressure $\sigma_{rr} = -p_o$, $a/b = 0.8$, $e/a = 1.05$, $k_n(e) = k(e)/p_o\sqrt{(g-e)/2}$, $k_n(g) = k(g)/p_o\sqrt{(g-e)/2}$.

$\frac{g-e}{b-a}$	$\lambda = 0$		$\lambda = 0.002$		$\lambda = 0.004$	
	$k_n(e)$	$k_n(g)$	$k_n(e)$	$k_n(g)$	$k_n(e)$	$k_n(g)$
0.05	4.3014	4.2703	4.3003	4.2693	4.2992	4.2684
0.10	4.3346	4.2662	4.3307	4.2633	4.3273	4.2606
0.20	4.4534	4.2872	4.4420	4.2800	4.4316	4.2734
0.30	4.6101	4.3256	4.5903	4.3156	4.5723	4.3064
0.40	4.7854	4.3935	4.7581	4.3828	4.7332	4.3730
0.50	4.9779	4.5473	4.9451	4.5382	4.9150	4.5297

Table 5. The stress intensity factor $k_n(g) = k(g)/q_o\sqrt{g-a}$ in a reinforced cylinder containing a radial crack which terminates at the interface (e=a, Figure 1). External load: crack surface pressure $q(r) = -q_o$, $a/b = 0.8$.

$\frac{g-a}{b-a}$	$\lambda = 0$	$\lambda = 0.002$	$\lambda = 0.004$
0.25	1.3380	0.8894	0.8701
0.30	1.4477	0.9256	0.9023
0.40	1.7159	0.9886	0.9580
0.50	2.0489	1.0375	1.0013
0.60	2.4352	1.0735	1.0345
0.70	2.8271	1.1065	1.0681

Table 6. Stress intensity factor $k_n(g) = k(g)/p_o\sqrt{g-a}$ in a pressurized reinforced cylinder containing a radial crack which terminates at the interface (e=a, Figure 1). External load: $\sigma_{rr}(a,0) = -p_o$, a/b = 0.8. (For the edge crack case, that is, for $\lambda = 0$ the effect of the pressure $\sigma_{\theta\theta}(r,0) = -p_o$ on the crack surfaces is not included). $(k_n^*(g) = k_n(g)/\sigma_{\theta\theta}(a,0)\sqrt{g-a})$

$\frac{g-a}{b-a}$	$\lambda = 0$ $k_n(g)$	$\lambda = 0$ $k_n^*(g)$	$\lambda = 0.002$ $k_n(g)$	$\lambda = 0.004$ $k_n(g)$
0.25	5.8477	1.2836	3.8533	3.7684
0.30	6.2838	1.3794	3.9755	3.8734
0.40	7.3578	1.6151	4.1768	4.0443
0.50	8.6933	1.9083	4.3154	4.1603
0.60	10.2352	2.2467	4.3977	4.2320
0.70	11.7739	2.5845	4.4642	4.3026

References

1. F. Delale and F. Erdogan, "Stress intensity factors in a hollow cylinder containing a radial crack", Int. Journal of Fracture, Vol. 20, 251 (1982).

2. F. Delale and F. Erdogan, "The crack problem for a half plane stiffened by elastic cover plates", Int. J. Solids Structures, Vol. 5, 381 (1982).

3. S. Krenk and M. Bakioglu, "Transverse cracks in a strip with reinforced surfaces," Int. J. Fracture, Vol. 3, 441 (1975).

4. J. Dundurs, "Elastic interaction of dislocations with inhomogeneities", in Mathematical Theory of Dislocations, T. Mura ed., 70 (1969).

5. R.W. Little, Elasticity, Prentice Hall (1973).

6. R.J. Tang and K. Wang, "On the Griffith crack whose surfaces are loaded asymmetrically", Engg. Fracture Mechanics, Vol. 16, 47 (1982).

7. F. Erdogan, "Mixed Boundary Value Problems in Mechanics", Mechanics Today, S. Nemat-Nasser, ed., Vol. 4, pp. 1-81, 1978, Vol. 6, pp. 199-202, 1981.

8. N.I. Maskhelishvili, Singular Integral Equation, P. Noordhoff, Groningen Holland (1953).

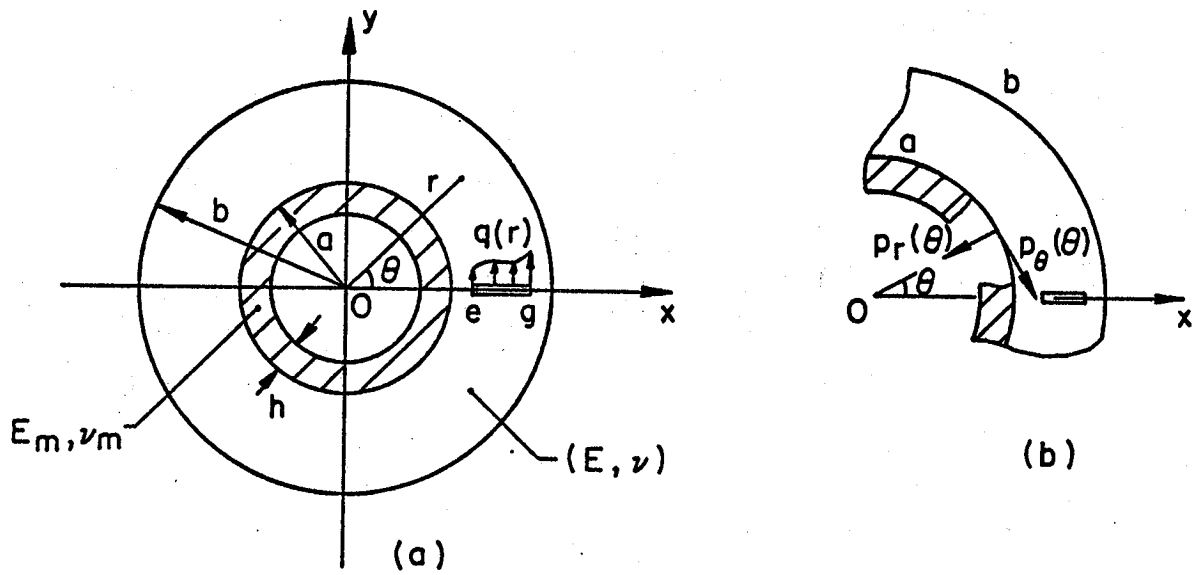

Figure 1. Geometry of a reinforced thick-walled cylinder containing a radial crack.

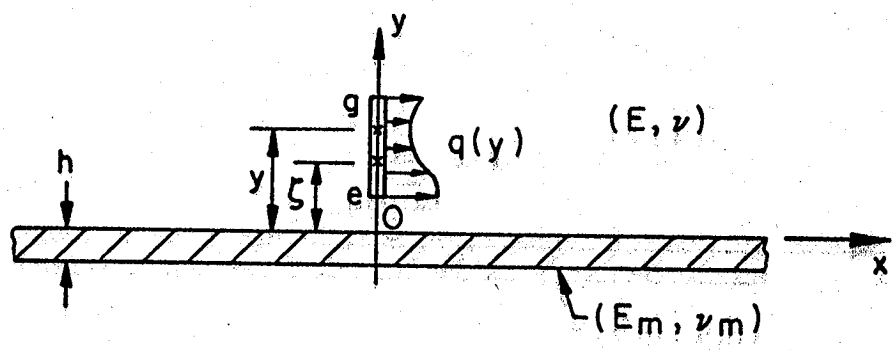

Figure 2. Notation for an elastic half plane which is reinforced by a membrane and which contains a finite crack.

1. Report No.	2. Government Accession No.	3. Recipient's Catalog No.
NASA CR-172307		

4. Title and Subtitle	5. Report Date
STRESS INTENSITY FACTORS IN A REINFORCED THICK-WALLED CYLINDER	February 1984
	6. Performing Organization Code
7. Author(s)	8. Performing Organization Report No.
Renji Tang and F. Erdogan	
9. Performing Organization Name and Address	10. Work Unit No.
Lehigh University Bethlehem, PA 18015	11. Contract or Grant No. NGR-39-007-011
12. Sponsoring Agency Name and Address	13. Type of Report and Period Covered
National Aeronautics and Space Administration Washington, DC 20546	Contractor Report
	14. Sponsoring Agency Code

15. Supplementary Notes

Langley technical monitor: W. S. Johnson

16. Abstract

In this paper an elastic thick-walled cylinder containing a radial crack is considered. It is assumed that the cylinder is reinforced by an elastic membrane on its inner surface. The model is intended to simulate pressure vessels with cladding. The formulation of the problem is reduced to a singular integral equation. Various special cases including that of a crack terminating at the cylinder-reinforcement interface are investigated and numerical examples are given. Among the interesting results found one may mention the following: In the case of the crack touching the interface, the crack surface displacement derivative is finite and consequently the stress state around the corresponding crack tip is bounded and, generally for realistic values of the stiffness parameter, the effect of the reinforcement is not very significant.

17. Key Words (Suggested by Author(s))	18. Distribution Statement
Elastic thick-walled cylinder Radial cracks Stress intensity factors	Unclassified - Unlimited Subject Category 39

19. Security Classif. (of this report)	20. Security Classif. (of this page)	21. No. of Pages	22. Price
Unclassified	Unclassified	25	A02

For sale by the National Technical Information Service, Springfield, Virginia 22161